Journal of Applied Physics

Features of streamer formation in a sharply non-uniform electric field

Cite as: J. Appl. Phys. **125**, 143301 (2019); https://doi.org/10.1063/1.5067294
Submitted: 17 October 2018 . Accepted: 01 March 2019 . Published Online: 10 April 2019

Dmitry A. Sorokin, Victor F. Tarasenko, Dmitry V. Beloplotov, and Mikhail I. Lomaev

Journal of Applied Physics ARTICLE scitation.org/journal/jap

Features of streamer formation in a sharply non-uniform electric field

Cite as: J. Appl. Phys. **125**, 143301 (2019); doi: 10.1063/1.5067294
Submitted: 17 October 2018 · Accepted: 1 March 2019 ·
Published Online: 10 April 2019

Dmitry A. Sorokin,[1,a)] Victor F. Tarasenko,[1,2] Dmitry V. Beloplotov,[1] and Mikhail I. Lomaev[1,2]

AFFILIATIONS

[1]Institute of High Current Electronics, Russian Academy of Science, Tomsk 634055, Russia
[2]National Research Tomsk State University, Tomsk 634050, Russia

[a)]SDmA-70@loi.hcei.tsc.ru

ABSTRACT

The streamer formation in a point-to-plane gap filled with atmospheric-pressure air has been experimentally studied using a streak camera and a four-channel intensified charge-coupled device camera with simultaneously recording waveforms of voltage and discharge current pulses. A large diameter streamer was observed at various amplitudes of nanosecond voltage pulses. The instantaneous streamer velocity was measured using the streak camera. It was found that the streamer has a high velocity at the initial stage of development, but it rapidly decreases. The minimum streamer velocity corresponds to the maximum diameter. The streamer velocity increases again by an order of magnitude when it approaches the opposite electrode. It was found that the streamer velocity correlates with the value of a displacement current induced by its propagation. At the initial stage of the streamer development during subnanosecond breakdown, the displacement current can reach several kiloamperes; this is comparable to the conduction current after the breakdown.

I. INTRODUCTION

Dense non-equilibrium low-temperature atmospheric-pressure plasma is an extremely promising tool for solving various problems of science and technology.[1–3] The simplest and most common method to produce such plasma is an electrical discharge in atomic and molecular gases (gas mixtures). Among them, volume discharges with an external preionization and diffuse discharges in a sharply non-uniform electric field should be noted.[4–6] Both types of the gas discharge produce the plasma with similar properties and parameters; however, there are differences in ignition methods and spatial structure.

To ignite the volume discharge, which is widely used in high-pressure gas lasers,[1] preliminary ionization of gas in the gap with a uniform electric field distribution is required. It is carried out using an external source of ionizing radiation (electron beam, X-rays, UV radiation, etc.). When the concentration of seeded electrons reaches $\sim 10^6$–$10^8\,\mathrm{cm}^{-3}$, electron avalanches overlap before they reach the critical size. As a result, the discharge occupies the whole space between the electrodes.[7] If the concentration of seeded electrons is insufficient, some avalanches can reach the critical size before overlapping. As a result, streamers with a small diameter ($\sim 100\,\mu$m) are formed. In a short time, they cross the gap and a spark channel with a high conductivity and a high temperature of heavy particles is formed.[8]

Diffuse discharges are formed in the gaps with a highly non-uniform electric field distribution.[6,9–11] In this case, there is no need to use external sources of ionizing radiation. Experimentally[12–16] and in simulations,[17,18] it was shown that a large-diameter plasma object, which we call "a streamer with a large diameter," develops in the gaps with a non-uniform electric field due to a high overvoltage. According to Ref. 19, its diameter can reach 8 cm. It has been reliably established that runaway electrons are generated in such discharges at the negative polarity of a pointed electrode.[6,11,20–23]

There are many research groups studying the features of the discharge development in the highly non-uniform electric fields.[6,12–19,24,25] However, the dynamics of the streamer development at different values of the breakdown delay time and voltage pulse polarities has not been fully studied. In particular, there are no data on the instantaneous streamer velocity v_{str} that develops in the non-uniform electric field. Nevertheless, it is known that the streamer velocity can change along the gap. In Ref. 24, it was found that v_{str} can vary by an order of magnitude during the propagation of streamers in the 16-cm-length gaps. A gradual increase in the streamer velocity in dielectric barrier discharges in short gaps with

a quasi-uniform electric field strength distribution was observed in experiments with a streak camera having an extremely high temporal resolution.[26–28] In Refs. 29 and 30, it was found that during the streamer development, the dynamic displacement current (DDC) caused by the electric field strength redistribution flows and it is measurable with a current shunt. The DDC could be also defined as the charging current of a capacitor formed by the streamer front and the opposite electrode. In Ref. 28, it was suggested that the value of the DDC depends on the streamer velocity. However, there are no experimental data on the instantaneous streamer velocity under these conditions. In addition, no studies on the dependence of the DDC value on the voltage pulse amplitude and the breakdown delay time have been carried out yet.

This paper presents the results of studies of the streamer formation in the highly non-uniform electric fields in atmospheric-pressure air at various voltages. Data on the instantaneous streamer velocity were obtained using the streak camera and a four-channel intensified charge-coupled device (ICCD) camera with simultaneous recording waveforms of the discharge current and voltage.

II. EXPERIMENTAL SETUP AND METHODS

The experimental studies were carried out on two setups (Fig. 1). The first one was designed to study the streamer formation by optical methods using a HSFC-PRO four-channel ICCD camera and a Hamamatsu C10910-05 streak camera. The ICCD camera allowed us to study the streamer formation with a simultaneous recording of voltage and current waveforms. The development of optical radiation along the discharge gap axis with a high temporal resolution was studied with the streak camera. The instantaneous streamer velocity at different voltages was estimated from the streak camera images.

GIN-50-1 ($U = 6$–25 kV, $\tau_{0.1-0.9} \approx 2.2$ ns, $\tau_{0.5} \approx 13$ ns, positive polarity) and GIN-55-01 ($U = 8$–35 kV, $\tau_{0.1-0.9} \approx 0.7$ ns, $\tau_{0.5} \approx 0.8$ ns, negative polarity) generators[31] were used on the first setup. Voltage pulses were applied to an electrode made of a 5-mm-length sewing needle 1 mm in diameter. The radius of the rounding of the needle tip was 75 μm. A grounded electrode was flat. Interelectrode distance d was 8.5 mm.

A capacitive voltage divider (CVD) and a current shunt made of surface mount resistors (SMD resistors) were used to measure voltage and current, respectively.

Electrical signals from the CVD, current shunt, as well as a clock signal from the first channel of the ICCD camera were recorded on a Tektronix TDS3054B oscilloscope (500 MHz, 5 GSa/s). These data were used to synchronize ICCD images and waveforms of voltage and current. The synchronization accuracy was ±0.5 ns.

The ICCD camera captured four consecutive images per pulse. While averaging, over 1000 pulses were required to obtain the streak image. Note that both the ICCD and the streak images are spectrally integrated. Furthermore, the emission bands of the second positive system of nitrogen molecules dominated the emission spectra. The streak camera was operated at various sweeps. The entrance slit (3 mm), which is perpendicular to the streak camera input slit (100 μm), was oriented so that the edges of the electrodes were aligned with its edges; adjustment was carried out in the "focus mode."

A SLEP-150 M generator (see Chapter 1 in Ref. 22) ($U = 200$ kV, $\tau_{0.1-0.9} \approx 0.25$ ns, $\tau_{0.5} \approx 1$ ns, switchable polarity) was used on the second setup. The generator was equipped with a 100-Ω transmitting line and a gas discharge diode. In general, the generator was designed to produce high-current (up to ~1 kA at a low gas pressure; see Chapter 6 in Ref. 22) electron beams. However, in these experiments, the generator was used to measure voltage and current under conditions of subnanosecond breakdown when applying 200-kV voltage pulses with a rise time of 0.25 ns across the gap. The waveforms were compared with those obtained on the first setup. As a result, some features of the discharge current were found under conditions when the streamer moves with a subluminal ($>2 \cdot 10^9$ cm/s) velocity.

Electrical signals from a capacitive voltage divider and a current shunt were recorded on an LeCroy WaveMaster 830Zi-A oscilloscope (30 GHz, 80 GSa/s). A tubular high-voltage electrode, like that on the first setup, was used. The d was varied from 8 to 16 mm.

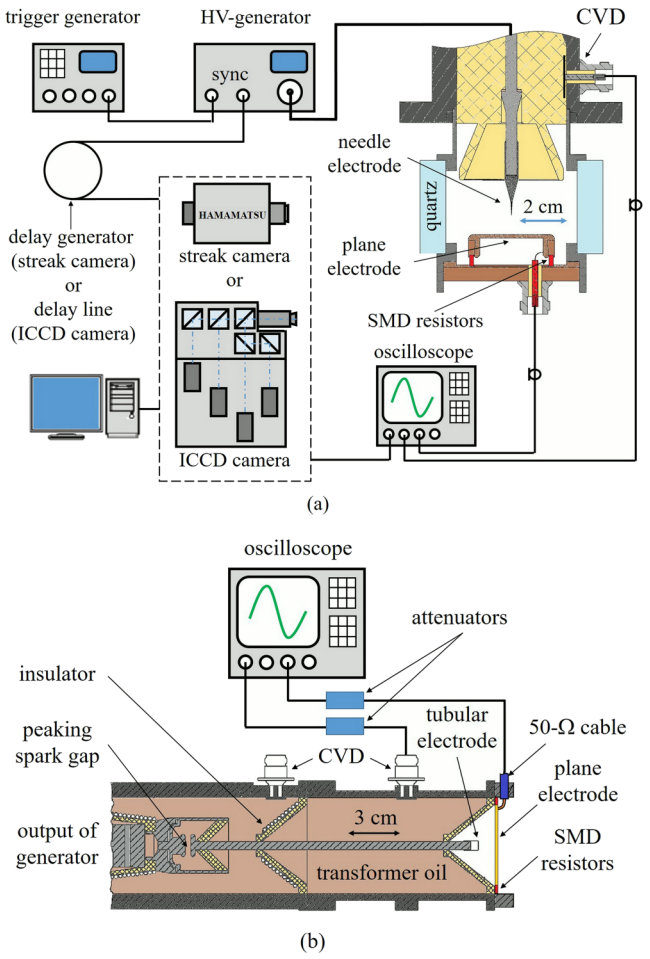

FIG. 1. Block diagram of experimental setups. (a) Setup 1 and (b) setup 2.

Note that because of the large jitter (~100 ns), it was impossible to use the ICCD and streak cameras on the second setup.

The discharge chambers on both setups were pumped out and then filled with air (humidity ≤30%) or nitrogen with the admixture concentration ≤0.001%. The gas pressure was 100 kPa.

III. RESULTS

The studies on setup 1 have been carried out at various voltages of positive polarity. The ICCD images of the discharge, as well as the corresponding waveforms of the voltage $U(t)$ and current $I(t)$, are presented in Figs. 2 and 3, respectively.

It can be seen that the streamer originates in the vicinity of the pointed electrode. Initially, it has the shape of a ball due to the initial distribution of the electric field strength in the gap. The distribution of the field along the gap axis is presented in Fig. 4. Simulation was performed with Elcut 4.1 software.

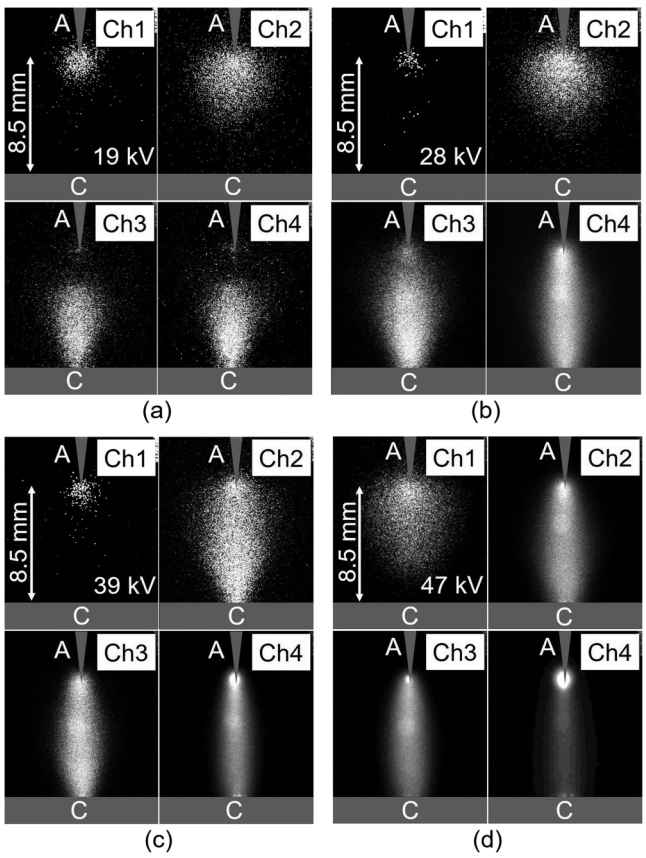

FIG. 2. ICCD images of the discharge in atmospheric-pressure air at various voltages. A: anode, C: cathode. Ch 1–Ch 4: channels of the four-channel ICCD camera. The moments of switching on the ICCD camera channels are presented in Fig. 3. Setup 1.

Large radius streamers are also observed in the simulations.[16,17] We consider that the inception clouds in Refs. 18 and 24 are also large streamers. As the streamer size increases [Figs. 2(a) and 2(b); Ch 2 and Fig. 2(d); Ch 1], the electric field strength at the streamer front decreases. At this stage, the highest electric field strength is reached in the axial zone because of less distance to the opposite electrode. As a result, the streamer develops faster in the direction of the opposite grounded electrode than in the radial direction and becomes narrow.

It is seen from Fig. 3 that a displacement current (*1*), the value of which is equal to the product of the capacitance C of the gap by the rate of voltage increase $dU(t)/dt$, is observed. When the streamer appears [Figs. 2(a)–2(c), Ch 1], a rapid increase (*2*) in a current is observed (Fig. 3). This is the DDC. It is well known that a time-varying electric field causes a displacement current. The emerging dense plasma redistributes the electric field in the gap. The electric field strength varies with time at each point in space, including that near the flat electrode (current shunt). The rate of change of the electric field strength obviously depends on the rate of filling the gap with the plasma or on the streamer velocity v_{str}. At a first approximation, it can be assumed that the DDC depends mainly on the streamer velocity; however, the change in its shape must also be taken into account. Figure 3(a) shows that the DDC decreases when the streamer reaches the largest radius [Fig. 2(a), Ch 2]. Then, the DDC increases again (*3*) when the streamer approaches the opposite grounded electrode [Fig. 2(a), Ch 3].

After bridging the gap, the conduction current flows predominantly through the gap. However, it should be noted that during the voltage fall, the current through the gap is the sum (*4*) of the conduction current and the displacement current $C \cdot dU(t)/dt$ flowing in the opposite direction [$dU(t)/dt < 0$] (Fig. 3).

Figure 3 also shows how the DDC changes with increasing voltage pulse amplitude. It is seen that the DDC increases and the time interval between peaks (*2*) and (*3*) decreases. When applying the maximum voltage across the gap [Fig. 3(d)], it was not possible to resolve (*2*) and (*3*) because of insufficient temporal resolution of the TDS 3053B oscilloscope (rise time is 0.7 ns). It should be noted that the DDC before the bridging the gap is comparable to that of the conduction current flowing through the gap after breakdown.

It should also be noted that at low voltages [Figs. 3(a) and 3(b)], breakdown of the gap does not lead to a noticeable voltage drop. It is assumed that this is due to the low conductivity of the plasma. At high voltages [Figs. 3(c) and 3(d)], the concentration of electrons is, probably, higher and the discharge current increases several times and the voltage across the gap drops.

Data on the $v_{str}(t)$ of positive streamers at various voltages were obtained on the first setup with the streak camera. Figure 5 shows streak images illustrating the temporal development of discharge emission at various voltage pulse amplitudes. A pulse repetition rate was 1 Hz. The images were taken at various sweeps: Figs. 5(a)–5(d) show the discharge emission dynamics at the initial stage, and Figs. 5(e)–5(h) show these during the entire voltage pulse. It should be noted that the streak images [Figs. 5(e)–5(h)] correlate with the ICCD images (Fig. 2) taken under the same conditions per one pulse. For example, the image presented in

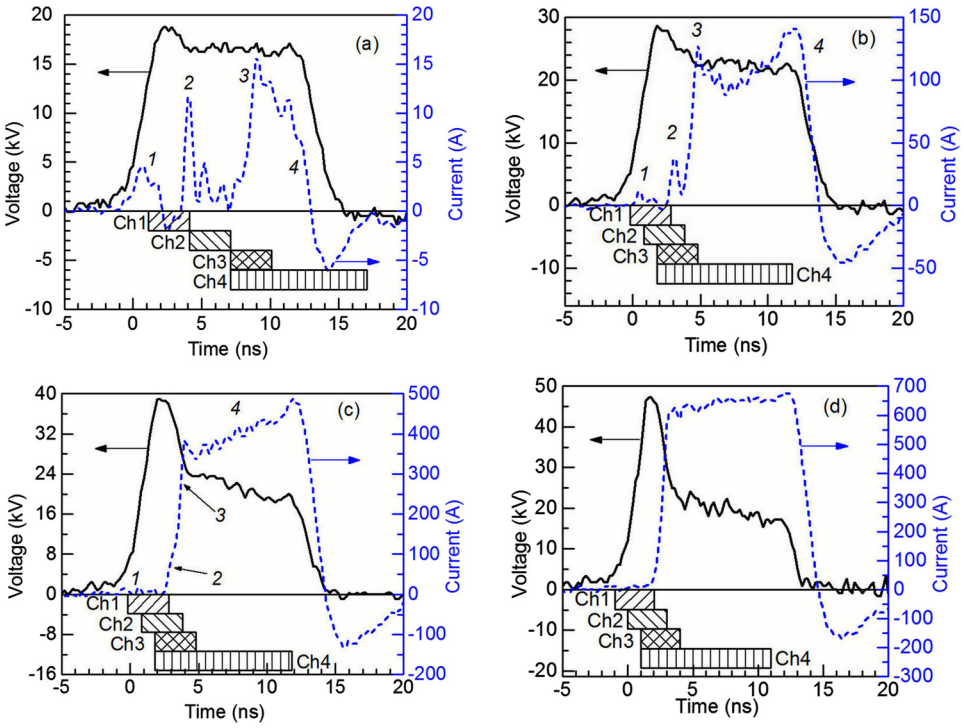

FIG. 3. Waveforms of the voltage and current at various voltage pulse amplitudes. *1*—displacement current $C{\cdot}dU(t)/dt$ [C—capacitance of the gap without plasma; $U(t)$—voltage]; *2*—dynamic displacement current caused by the rapid redistribution of the electric field when the streamer emerges. *3*—dynamic displacement current caused by the rapid redistribution of the electric field as a result of streamer acceleration before the gap bridging; *4*—sum of the conduction current and the displacement current caused by the changes in $U(t)$. Ch 1–Ch 4: channels of the four-channel ICCD camera; the moments of switching on and gate widths are shown by rectangles. Setup 1.

Fig. 2(a), channel 4, corresponds to the streak image presented in Fig. 5(e) (a time interval of 6–16 ns).

It is seen from Figs. 5(a)–5(e) that the streamer front propagates along the gap at various velocities. Time resolution at 16-ns sweeps [Figs. 5(f)–5(h)] is insufficient to observe changes in the streamer velocity. Note that it is difficult to objectively determine the position of the streamer front because of the graininess of the image. However, as we will see below, this was not so critical and the streak images allow roughly $v_{str}(t)$.

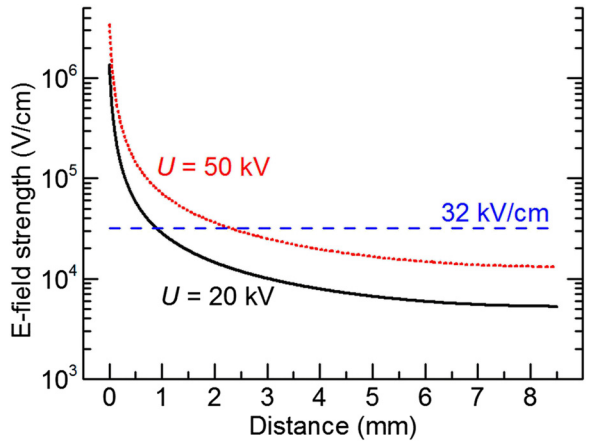

FIG. 4. Electric field strength distribution in the 8.5-mm point-to-plane gap at various voltages. The dashed blue line corresponds to the threshold electric field for the breakdown of atmospheric-pressure air in a quasistatic electric field. Setup 1.

Figure 6 shows how the streamer velocity was estimated.

Two envelope curves (*1*) and (*2*) in Fig. 6(a) show the location of the streamer front. These curves were digitized by Graph2Digit 0.7.1b software and then the time derivative was calculated. The result of the calculation is the streamer velocities $v_1(t)$ and $v_2(t)$ [Fig. 6(c)]. The velocities $v_1(t)$ and $v_2(t)$ differ noticeably (1.5–2 times) only at the initial stage of streamer development. The mean values of v_1 and v_2 are 0.16 and 0.15 cm/ns, respectively. The same procedure was performed with the streak image in Fig. 6(b); the mean streamer velocity is 0.14 cm/ns. Greatest $v_{str}(t)$ is observed when the streamer starts from the high-voltage needle, as well as when it approaches the opposite electrode (Fig. 6).

The mean streamer velocity (v_{DDC}) can also be estimated from the current waveform in Fig. 3(a); the propagation time of the streamer along the 8.5-mm gap is the difference in time between *2* and *3* in Fig. 3(a) ($\Delta t \approx 5$ ns). As a result, $v_{\mathrm{DDC}} = 0.17$ cm/ns.

Figure 7 shows $v_{str}(t)$ for other voltages.

According to the presented dependencies, at the initial stage, the streamer velocity reaches 0.5–2 cm/ns, depending on the voltage amplitude. Then, as the streamer develops, v_{str} rapidly decreases by a factor of 5–10. The minimum v_{str} is observed when the streamer crosses ≈60%–70% of the gap [Figs. 5(a)–5(e) and 6].

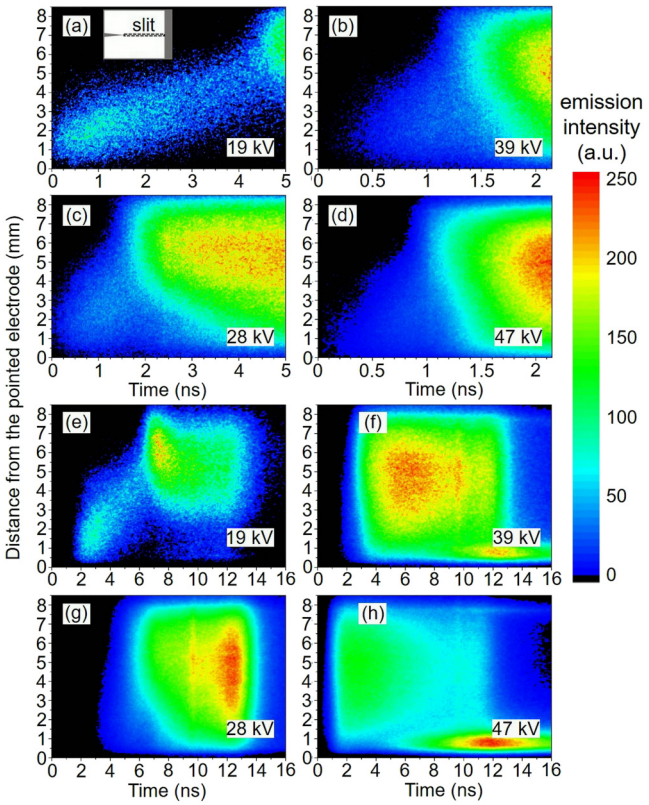

FIG. 5. Streak images of the discharge emission in atmospheric-pressure air at various voltages of positive polarity as well as at various sweeps. Setup 1.

The maximum v_{str} is observed when the streamer approaches the opposite electrode. The result obtained is similar to that reported in Ref. 24; the formation of streamers in a 160-mm point-to-plane gap filled with artificial air at a pressure of ≈10 kPa was studied. The time behavior of $v_{str}(t)$ (Fig. 6) is correlated with DDC (Fig. 3).

It should be noted that the mean v_{str} is 3–5 times less than the maximum one. The mean streamer velocities estimated from both the DDC (Fig. 3) and the streak images (Fig. 5) at various voltages are presented in Table I.

Figure 8 shows the waveforms of the voltage and current as well as the time-integrated image of a discharge emission obtained on the second setup [Fig. 1(b)].

A significant increase in the amplitude ($U_0 \approx 200$ kV) and a decrease in the rise time (up to 0.3 ns) of voltage pulses lead to an increase in v_{str} by a factor of 3–5. Under these conditions, at negative polarity, a runaway electron beam with a current amplitude of $\sim 10^1$–10^2 A is generated.[20,22]

Due to the short rise time, the displacement (capacitive) current (*1*) with an amplitude of up to 500 A flows in the gap [Figs. 8(a) and 8(b)]. At $d = 8$ mm, the DDC is observed during the voltage pulse rise. The DDC reaches ≈3–4 kA. This indicates the high streamer velocity. The conduction current after the breakdown can be modulated by both direct and inverse displacement currents caused by voltage changes. At $d = 16$ mm, the streamer velocity is less, and (*2*) and (*3*) in Fig. 8(b) are distinguishable. This allows a rough estimate of v_{DDC}—≈8 cm/ns. This value is an order of magnitude higher than that in Table I.

It is seen from Figs. 8(a) and 8(b) that the DDC is comparable to the conduction current flowing after breakdown. Moreover, when the streamer starts, the DDC reaches half the amplitude of the discharge current after the breakdown.

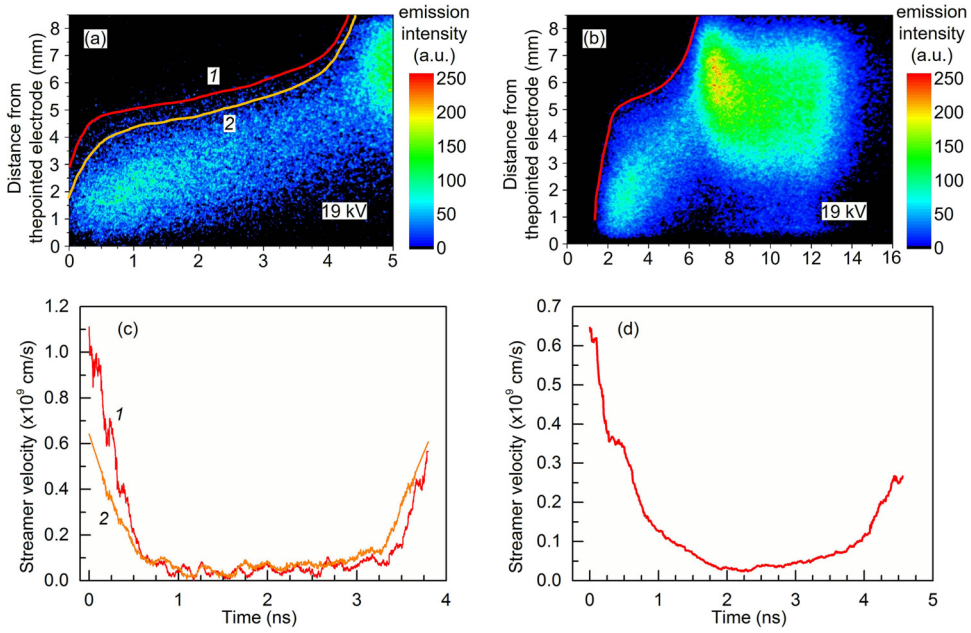

FIG. 6. (a) and (b) Examples of determining the streamer front position on the streak image at various sweeps. (c) and (d) Streamer velocities calculated from the corresponding streak images. *1* and *2*—various profiles of the streamer front. Setup 1.

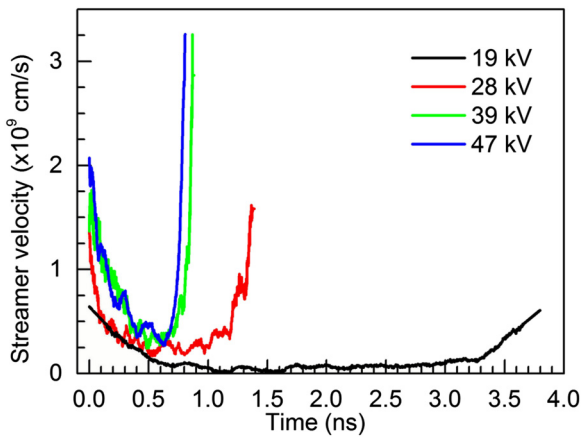

FIG. 7. Streamer velocities calculated from the streak images taken at various voltages. Setup 1.

IV. DISCUSSION

The result shows that the diffuse discharge is formed in the gap with the highly non-uniform electric field strength distribution without the use of external sources of ionizing radiation. The highly non-uniform electric field strength distribution significantly affects the dynamics of the streamer development. The results obtained differ qualitatively from the results of studying the development of a positive streamer in a quasi-uniform electric field between semi-spherical electrodes covered with a dielectric (dielectric barrier discharge) presented in Refs. 26–28 where similar optical diagnostics were applied. The results show that in the quasi-uniform electric field, the positive streamer develops without any features in its velocity. The streamer velocity increases gradually as the distance between the streamer and the opposite electrode decreases. Furthermore, a long Townsend-phase precedes the streamer appearance. In the point-to-plane gap, the avalanche-to-streamer transition occurs quickly (up to several hundreds of ps) due to the enhancement of the electric field near the pointed electrode (≥1 MV/cm near the electrode surface, Fig. 4). The characteristic length when an avalanche reaches the critical size is ~0.1 mm. Furthermore, at positive polarity, initial electrons in the point-to-plane gap are produced, most likely, by accelerated ions that appear as a result of an autoionization of molecules and atoms on the surface of the pointed electrode (anode) due to the high electric field strength. This is supported by the fact that the statistical lag and breakdown voltage decreases with an increase in the electrode tip roughness; the electric field strength is enhanced by microprotrusions.

TABLE I. The mean streamer velocities (cm/ns) estimated from both the DDC and the streak images at various voltages.

Voltage	19 kV	28 kV	39 kV	48 kV
From DDC	0.17	0.5	0.7	–
From streak images	0.15–0.16	0.45	0.75	0.8

At the initial stage of the streamer development, the electric field strength at its front is high, and electric field lines diverge from its surface like a "fan." As a result, the streamer front moves in all directions and becomes spherical [Figs. 2(a) and 2(b); Ch 1 and Ch 2] as in simulations.[17] Similar plasma formations are also observed in simulations.[18,32] During the streamer development, its velocity changes significantly (Figs. 6 and 7). The streamer velocity decreases rapidly with an increase in its radius due to a rapid decrease in the electric field strength at its front. The dynamics of the positive streamer development in our experiments coincides well with the results of modeling[33] a negative streamer, but it differs for a positive one.

Features of the streamer velocity change in a curious way affect the discharge current. The rapid formation of a dense plasma in the gap leads to the flow of the DDC. The time behavior of DDC is correlated with $v_{str}(t)$ and depends on the voltage across the gap (Figs. 3 and 7). During subnanosecond breakdown, the DDC is comparable to the current flowing after the breakdown.

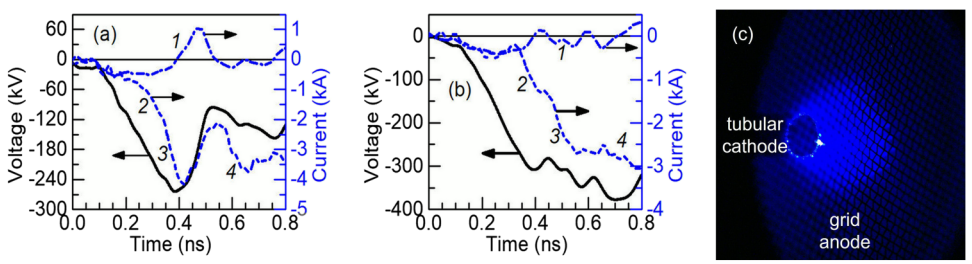

FIG. 8. (a) and (b) Waveforms of the voltage and discharge current through the gap for $d = 8$ and 16 mm, respectively. *1*—displacement current $C \cdot dU(t)/dt$ [C—capacitance of the gap without plasma; $U(t)$—voltage]; *2*—dynamic displacement current caused by the rapid redistribution of the electric field when the streamer emerges; *3*—dynamic displacement current caused by the rapid redistribution of the electric field as a result of streamer acceleration before the gap bridging; *4*—sum of the conduction current and displacement current caused by the changes in $U(t)$. (c) Time-integrated image of the discharge. Setup 2.

V. CONCLUSION

The streamer formation in the sharply non-uniform electric field at various voltages has been experimentally studied with the four-channel ICCD and streak cameras. It was found that the streamer velocity rapidly decreases by 5–10 times after its appearance due to an increase in its diameter. The mean values of streamer velocities are 3–5 times less than the maximum ones. A decrease in the distance to the opposite electrode and in the radius of curvature of the streamer head leads to an increase in the streamer velocity.

It was found that the time behavior of the streamer velocity correlates with the DDC. By measuring the DDC, it is possible to find the mean streamer velocity. It was shown that the mean streamer velocities measured by the DDC and the streak camera are very close. It is of interest to find a direct relationship between the magnitude of the DDC and the streamer velocity in order to measure its instantaneous values by a simple measurement of the current.

The DDC can reach values comparable to the discharge current after the breakdown. From this point of view, the gap can be considered broken down before it is completely bridged by the plasma. As for the subnanosecond breakdown, the gap can be considered broken down as soon as the streamer begins to develop. If we consider the gas-discharge gap as a switch, then a noticeable voltage appears on a load even before the gap is completely bridged by the plasma.

ACKNOWLEDGMENTS

This work was performed with the support of a grant from the Russian Science Foundation (Project No. 17-72-20072).

REFERENCES

[1]G. A. Mesyats, V. V. Osipov, and V. F. Tarasenko, *Pulsed Gas Lasers* (SPIE Press, 1995).
[2]R. Hippler, H. Kersten, M. Schmidt, and K. H. Schoenbach, in *Low Temperature Plasma Fundamentals, Technologies, and Techniques* (Wiley-VCH Verlag GmbH&Co., 2008).
[3]P. K. Chu and X. Lu, in *Low Temperature Plasma Technology* (CRC Press, 2014).
[4]Y. D. Korolev and G. A. Mesyats, *Physics of Pulsed Breakdown in Gases* (URO-Press, 1998).
[5]V. V. Osipov, Phys.-Uspekhi **43**(3), 221 (2000).
[6]V. F. Tarasenko, in *Runaway Electrons Preionized Diffuse Discharges* (Nova Science, 2014).
[7]A. J. Palmer, Appl. Phys. Lett. **25**(3), 138 (1974).
[8]Y. D. Korolev and G. A. Mesyats, *Field-Emission and Explosive Processes in Gas Discharges* (Nauka, 1982).
[9]R. C. Noggle, E. P. Krider, and R. J. Wayland, J. Appl. Phys. **39**(10), 4746 (1968).
[10]L. V. Tarasova and L. N. Khudyakova, Sov. Phys. Tech. Phys., Engl. Transl. **14**(8), 1148 (1969).
[11]L. P. Babich, *High-Energy Phenomena in Electric Discharges in Dense Gases: Theory, Experiment and Natural Phenomena* (Futurepast, 2003).
[12]A. Y. Starikovskiy, IEEE Trans. Plasma Sci. **39**(12), 2602 (2011).
[13]S. Yatom, V. Vekselman, J. Z. Gleizer, and Y. E. Krasik, J. Appl. Phys. **109**(7), 073312 (2011).
[14]P. Tardiveau, N. Moreau, S. Bentaleb, C. Postel, and S. Pasquiers, J. Phys. D Appl. Phys. **42**, 175202 (2009).
[15]P. Tardiveau, L. Magne, E. Marode, K. Ouaras, P. Jeanney, and B. Bournonville, Plasma Sources Sci. Technol. **25**(5), 054005 (2016).
[16]G. V. Naidis, V. F. Tarasenko, N. Y. Babaeva, and M. I. Lomaev, Plasma Sources Sci. Technol. **27**(1), 013001 (2018).
[17]N. Y. Babaeva and G. V. Naidis, Phys. Plasmas **23**(8), 083527 (2016).
[18]J. Teunissen and U. Ebert, Plasma Sources Sci. Technol. **25**(4), 044005 (2016).
[19]V. F. Tarasenko, G. V. Naidis, D. V. Beloplotov, I. D. Kostyrya, and N. Y. Babaeva, Plasma Phys. Rep. **44**(8), 746 (2018).
[20]V. F. Tarasenko, E. K. Baksht, A. G. Burachenko, I. D. Kostyrya, M. I. Lomaev, and D. V. Rybka, Plasma Devices Oper. **16**(4), 267 (2008).
[21]T. Shao, C. Zhang, Z. Niu, P. Yan, V. F. Tarasenko, E. K. Baksht, A. G. Burachenko, and Y. V. Shut'ko, Appl. Phys. Lett. **98**(2), 021503 (2011).
[22]V. F. Tarasenko, "Generation of runaway electron beams and X-rays in high pressure gases," in *Techniques and Measurements* (Nova Science Publishers, Inc., 2016), Vol. 1.
[23]G. A. Mesyats, M. S. Pedos, S. N. Rukin, V. V. Rostov, I. V. Romanchenko, A. G. Sadykova, K. A. Sharypov, V. G. Shpak, S. A. Shunailov, M. R. Ul'masculov, and M. I. Yalandin, Appl. Phys. Lett. **112**(16), 163501 (2018).
[24]S. Chen, L. C. J. Heijmans, R. Zeng, S. Nijdam, and U. Eber, J. Phys. D Appl. Phys. **48**, 175201 (2015).
[25]V. F. Tarasenko, "Generation of runaway electron beams and x-rays in high pressure gases," in *Processes and Applications* (Nova Science Publishers, Inc., 2016), Vol. 2.
[26]R. Brandenburg, M. Bogaczyk, H. Höft, S. Nemschokmichal, R. Tschiersch, M. Kettlitz, L. Stollenwerk, T. Hoder, R. Wild, K.-D. Weltmann, J. Meichsner, and H.-E. Wagner, J. Phys. D Appl. Phys. **46**, 464015 (2013).
[27]H. Höft, M. Kettlitz, M. M. Becker, T. Hoder, D. Loffhagen, R. Brandenburg, and K.-D. Weltmann, J. Phys. D Appl. Phys. **47**, 465206 (2014).
[28]H. Höft, M. M. Becker, and M. Kettlitz, Plasma Sources Sci. Technol. **27**, 03LT01 (2018).
[29]D. V. Beloplotov, M. I. Lomaev, V. F. Tarasenko, and D. A. Sorokin, JETP Lett. **107**(10), 606 (2018).
[30]T. Shao, V. F. Tarasenko, C. Zhang, A. G. Burachenko, D. V. Rybka, I. D. Kostyrya, M. I. Lomaev, E. K. Baksht, and P. Yan, Rev. Sci. Instrum. **84**(5), 053506 (2013).
[31]V. M. Efanov, M. V. Efanov, A. V. Komashko, A. V. Kirilenko, P. M. Yarin, and S. V. Zazoulin, *Ultra-Wideband, Short Pulse Electromagnetics 9. Part 5.* (Springer, 2010).
[32]F. Pechereau, P. L. Delliou, J. Jansky, P. Tardiveau, S. Pasquiers, and A. Bourdon, IEEE Trans. Plasma Sci. **42**(10), 2346 (2014).
[33]A. Luque, V. Ratushnaya, and U. Ebert, J. Phys. D Appl. Phys. **41**, 234005 (2008).